

1 **Rainfall redistribution in subtropical Chinese forests changes over 22**
2 **years**

3 Wanjun Zhang^{a,b,c}, Thomas Scholten^c, Steffen Seitz^c, Qianmei Zhang^a, Guowei Chu^a, Linhua Wang^a,
4 Xin Xiong^{d,*}, Juxiu Liu^{a,*}

5
6 ^a*Key Laboratory of Vegetation Restoration and Management of Degraded Ecosystems, South China*
7 *Botanical Garden, Chinese Academy of Sciences, Guangzhou, 510650, China*

8 ^b*Key Laboratory of Urban Water Safety Discharge and Resource Utilization, Hunan University of*
9 *Technology, Zhuzhou, 412007, China*

10 ^c*Soil Science and Geomorphology, Department of Geosciences, University of Tübingen, Tübingen,*
11 *72070, Germany*

12 ^d*Lushan Botanical Garden, Chinese Academy of Sciences, Jiujiang 332900, China*

13

14 * Correspondence to: Juxiu Liu (ljxiu@scbg.ac.cn) and Xin Xiong (xiongx@lsbg.cn)

15 **Abstract**

16 Rainfall redistribution through the vegetation canopy plays a key role in the
17 hydrological cycle. Although there have been studies on the heterogeneous patterns of
18 rainfall redistribution in some ecosystems, the understanding of this process in different
19 stages of forest succession remains insufficient. Therefore, this study investigated the
20 change tendency of rainfall redistribution and rainwater chemistry in a subtropical
21 succession forest area in South China, based on 22 years (2001–2022) of monitoring
22 740 valid rainfall events. Results showed that at the event scale throughfall ratio showed
23 in order broadleaf forest (BF) < mixed forest (MF) < pine forest (PF), and stemflow
24 ratio showed in order BF > MF > PF. At the interannual scale, throughfall and stemflow
25 of forests experienced a decreasing followed by an increasing from 2001–2022 (except
26 stemflow of the pine forest), similar with the trend of open rainfall (except the mutation
27 time). The variability of throughfall presented in order MF (CV, 9.7%) < PF (11.8%) <
28 BF (16.4%), and variability of stemflow presented in order MF (CV, 38.6%) < PF (50.9)
29 < BF (56.2%). This suggested that changes of throughfall and stemflow in the broadleaf
30 forest were greater than those in the mixed forest and pine forest over time. annual gross
31 rainfall considerably shifted over time, which directly induced the variable
32 accumulation of annual throughfall and annual stemflow. In the last 22 years, annual
33 variability of throughfall presented in order MF (CV, 9.7%) < BF (15.6%) < PF (16.1%),
34 and annual variability of stemflow presented in order MF (CV, 38.6%) < PF (50.9) <
35 BF (56.2%). The spatial variability of stemflow was always greater than that of
36 throughfall. Besides, the difference of rainwater chemistry fluxes (TN, TP and K⁺)
37 among the three forest types were found and they changed in different order over time.
38 ~~Throughfall was characterized with high chemistry fluxes compared to open rainfall~~
39 ~~followed by stemflow.~~ On average, TN and TP fluxes of throughfall presented in order
40 BF < MF < PF, while K⁺ flux of throughfall presented in order BF > MF > PF. Stemflow
41 chemical fluxes varied less among forest types and/or over time, though tree species
42 exactly contribute to differences in stemflow chemistry. The above results indicated that
43 the patterns of rainfall redistribution ~~often~~ changed over time and showed characteristic
44 variation driven by rainfall and forest factors. ~~The event scale accumulation of~~
45 ~~throughfall and stemflow potentially induced the interannual scale variability. Both~~
46 ~~water volume and chemistry of throughfall and stemflow depended on the effect of~~
47 ~~rainfall and forest factors.~~ This study provided insight into the rainfall redistribution
48 process by linking the long-term changing of rainfall pattern and subtropical forest

49 succession sequence.

50 **Keyword:** throughfall, stemflow, variability, forest types, long-term

51 **1. Introduction**

52 In recent years, there has been on-going concern about the potential impacts of
53 climate change on forest ecosystems, particularly in terms of rainfall input associated
54 to water resource (Reynaert et al., 2020; Grossiord et al., 2017; Bruijnzeel et al., 2011;
55 Leuzinger and Körner, 2010). Numerous studies have documented rainfall regimes and
56 their effect on the water cycle in different regions of the world, including spatial and
57 temporal changes in the amount, intensity, and frequency (Brasil et al., 2018; Ponette-
58 González et al., 2010). Meanwhile, these variables in rainfall refer to the redistribution
59 of rainfall into canopy interception, throughfall and stemflow, being important
60 components of terrestrial ecosystems hydrological processes (Germer et al., 2010;
61 Levia and Frost, 2006; Loustau et al., 1992). Rainfall redistribution patterns can impact
62 the biogeochemistry cycle by affecting soil moisture distribution, which in turn affects
63 the activity of soil microorganisms that decompose organic matter (Tonello et al., 2021a;
64 Junior et al., 2017; Van Stan II and Pypker, 2015). The study of Sun et al. (2023) verified
65 that throughfall reduction significantly affected soil carbon cycle in a subtropical forest.
66 Therefore, understanding the roles of rainfall redistribution in the water cycle is
67 essential.

68 Rainfall redistribution, as the partitioning into interception loss, throughfall and
69 stemflow, is an important hydrological process that regulates water and nutrient cycling
70 in forest ecosystems. Interception loss refers to the part of the event rainfall intercepted
71 by the canopy, accounting for about 10%–30% of gross rainfall depending on the
72 studied forest canopy, such as shrub (Zhang et al., 2015), mixed broadleaf (Yan et al.,
73 2003), pine (Loustau et al., 1992). ~~This portion of the rainwater evaporates directly back~~
74 ~~into the atmosphere.~~ Later on, the remaining rainwater reaches the ground either as
75 throughfall or stemflow. Throughfall is a critical component of rainfall redistribution,
76 and it on average contributes to approximately 60%–90% of the gross rainfall on the
77 floor in forests, shrubland or cropland. (Zhang et al., 2023; Zhang et al., 2021; Brauman
78 et al., 2010; Marin et al., 2000). Raindrops coalesce or splash on canopy leaf surfaces,
79 generating spatially different throughfall volume and raindrop kinetic energies which
80 can be larger or lower than that of open rainfall (Levia et al., 2019; Goebes et al., 2015).
81 Stemflow, the left rainwater flowing bottomwards along the plant stem or trunk, often
82 accounts for only a small proportion (0–12%) of rainfall (Niu et al., 2023; Yue et al,
83 2021; Llorens and Domingo 2007). Nevertheless, stemflow inputs can be important as
84 hot spots for near-trunk soils, inducing water and nutrient enrichment and deep

85 infiltration, but also erosion (Zhao et al., 2023; Llorens et al., 2022). It can funnel more
86 water than open rainfall on an equivalent area and contributes to 10% of the annual soil
87 water input (Levia and Germer, 2015; Chang and Matzner, 2000). Throughfall and
88 stemflow restrict water input to the soil layer, thereby affecting soil moisture conditions,
89 runoff generation and water and nutrient cycling ([Lian et al., 2022](#); Lacombe et al.,
90 2018; Klos et al., 2014).

91 The proportions of rainfall redistribution are generally driven by meteorological
92 conditions (e.g., rainfall amount, intensity, duration) and vegetation cover (e.g., canopy
93 structures, tree characteristics) (Tonello et al., 2021a; Sun et al., 2018; Muzyło et al.,
94 2012; Nanko et al., 2006). For meteorological conditions, numerous studies have
95 documented that throughfall volume and stemflow volume increase with increasing
96 gross rainfall and intensity (Ji et al., 2023; André et al., 2011). The ratios of throughfall
97 and stemflow were both characterized with logarithmically increasing with rainfall,
98 tending to be quasi-constant for heavy rainfall events (Zhang et al., 2021; Liu et al.,
99 2019). This was also synchronously related to the gradual saturation of the canopy
100 which limited the ratios of rainwater partitioning (Carlyle-Moses et al., 2004). Besides,
101 differences of water volume spatially exist from place to place. The spatial variability
102 (expressed as a coefficient of variation) of throughfall volume is generally higher for
103 small rainfall events (< 10 mm) than that for heavy rainfall events (Germer et al., 2006;
104 Price et al., 1997).

105 Rainfall redistribution among different plant species can vary significantly due to
106 differences in the structure and characteristics of their canopies. In special, some of the
107 key factors determine the redistribution of rainfall, for example, leaf area index (LAI),
108 leaf shapes and orientations can affect the amount of intercepted loss and throughfall
109 (Zhang et al., 2021; Goebes et al., 2015; Keim et al., 2006). The diameter at breast
110 height (DBH), bark type and orientation of trunks/stems and branches influence the
111 amount of stemflow (Levia et al., 2015; Livesley et al., 2014; Germer et al., 2010). For
112 each of the rainfall partitioning fluxes, their responses to the influential predictors often
113 show high variation. A modelling study of rainfall partitioning in China explained that
114 throughfall was best represented by mean tilt angle (MTA), followed by DBH.
115 Subsequently, DBH was the dominant predictor for stemflow, followed by LAI and
116 bark texture (Zhang et al., 2023). Due to these factors, rainfall redistribution presented
117 different degrees of spatial variability. This variability (expressed as coefficient of
118 variation) decreased with increasing rainfall amount and intensity, consequently

119 tending to be quasi-constant (Germer et al., 2006). Besides, at interannual scale, ratios
120 of rainfall redistribution are driven by annual canopy structures. The study of Niu et al.
121 (2023) documented that annual throughfall ratio gradually increased, while annual
122 stemflow ratio and interception loss ratio decreased with increasing thinning intensity
123 in shrub plantation. Meanwhile, annual changes of rainfall events (amount and intensity)
124 reinforced the time instability of throughfall spatial variability (Rodrigues et al., 2022).
125 Overall, the rainfall-canopy interactions play a key role in rainfall redistribution
126 processes and further affect the water cycle in many ecosystems.

127 Vegetation canopy is the functional interface between ecosystem and atmospheric
128 wet deposition (Van Stan II and Pypker, 2015). The leaf and trunk/stem, acting as a
129 filter, alter rainwater chemical concentrations via leaching and depositing processes. As
130 a result, throughfall and stemflow exhibit high chemical concentrations compared to
131 the open rainfall (Jiang et al., 2021; Zimmermann et al., 2007). For instance, in a Chinese
132 pine plantation, the volume weighted mean concentrations of NH_4^+ and NO_3^- in
133 throughfall were significantly higher than those in open rainfall (Wang et al., 2023).
134 Stemflow ion fluxes (e.g., K^+) from deciduous tree species were greater than those for
135 evergreen tree species because of the differences in bark morphology and branch
136 architecture (Su et al., 2019). Moreover, it is also common that throughfall and
137 stemflow chemistry fluctuated seasonality with the shifts in rainfall regime and leaf
138 growth (Turpault et al., 2021; Siegert and Levia, 2014; Staelens et al., 2007). A large
139 number of elements required by plants are mainly N, P, K, Ca and Mg. In general, N, K
140 and Ca are the most important inputs to forest ecosystem, and P is the least. Phosphorus
141 (P) is considered to be a limiting nutrient element in tropical and subtropical forests.
142 The long-term productivity of vegetation depends on the input of atmospheric P.
143 Besides, the increasing trend in seasonal drought and atmospheric nitrogen (N)
144 deposition in subtropical areas of China were reported (Zhou et al., 2011), and may
145 inhibit the growth of plant and affect productivity and functioning of forest ecosystems
146 (Wu et al., 2023; Borghetti et al., 2017). Therefore, the important significance of
147 atmospheric precipitation to the ecosystem can also be seen from the amount of element
148 cycling, and canopy leaching also plays an important role in the chemistry cycle of
149 forest ecosystems.

150 Although there have been studies on the spatio-temporal variability of rainfall
151 redistribution, most of these are limited to data of short-term monitoring over one-two
152 years or several months (Liu et al., 2019; Ziegler et al., 2009; Carlyle-Moses, 2004;

153 Marin et al., 2000). There are few studies exceeding several years experiments and
154 focusing on forest structural changes and rainwater interception (Grunicke et al., 2020;
155 Shinohara et al., 2015; Jackson, 2000). Long-term field monitoring studies are
156 considered to be valuable to gain insight into the temporal dynamics of forest
157 hydrological processes (Rodrigues et al., 2022; Sun et al., 2023; Levia and Frost, 2006).
158 Such studies can also contribute to identify patterns and trends in rainfall redistribution,
159 which is essential for predicting the long-term effect of water resource change on forest
160 ecosystems.

161 Therefore, in this study, we focus on the changing characteristics of throughfall
162 and stemflow in a subtropical forest succession sequence (pine forest→mixed forest→
163 monsoon evergreen broadleaf forest), based on long-term monitoring. Specifically, the
164 objectives are to analyze: (1) the changes of water volume of throughfall and stemflow
165 among the three forests, (2) the changes of water chemistry (TN, TP, K⁺) of rainfall,
166 throughfall and stemflow among the three forests. We hypothesize that: (1) both
167 throughfall and stemflow in the broadleaf forest were characterized with high
168 variability compared to mixed forest followed by pine forest, (2) chemistry flux of
169 throughfall and stemflow changed over time with in order broadleaf forest > mixed
170 forest > pine forest. We aim to assess the variability of forest hydrological processes
171 from a long-term perspective to help predict future dynamic trends of water resources
172 in subtropical forest ecosystems.

173

174 **2. Materials and Methods**

175 *2.1. Study site*

176 This study was conducted at the Dinghushan Biosphere Reserve (23°09' 21" N ~
177 23°11' 30" N, 112°30' 39" E ~ 112°33' 41" E) located in Zhaoqing City, South China.
178 Dinghushan catchment consists of two streams both with 12 km length, which flow into
179 the West River (the main trunk of the Pearl River). According to the Köppen-Geiger
180 climate classification (Kottek et al., 2006), the study area belongs to tropical monsoon
181 climate (Cwa) with pronounced wet (April-September) and dry season (October-
182 March). The average annual temperature is 20.9 °C, and the annual rainfall and
183 evaporation are 1900 mm and 1115 mm, respectively. Dinghushan Biosphere Reserve
184 is covered with a complete horizontal succession series of three types of subtropical
185 forest, which is highly representative of the region (Zhou et al., 2011). Monsoon

186 evergreen broadleaf forest (BF) is 400 years old with typical tree species including
187 *Castanopsis chinensis* (Spreng.) Hance, *Schima superba* Gardner & Champ.,
188 *Cryptocarya concinna* Hance, etc. The mixed pine/broadleaf forest (MF) is a natural
189 succession with a coniferous broadleaf ratio of about 4:6, and 70–80 years old. The
190 main broadleaf tree species are *Schima superba* Gardner & Champ., *Castanopsis*
191 *chinensis* (Spreng.) Hance, and the coniferous species *Pinus massoniana* Lamb. The
192 pine forest (PF) planted before 1960 belongs to the primary succession community
193 where *Pinus massoniana* Lamb forms the only tree layer. The community composition
194 and biodiversity are shown in Table S1.
195

196 2.2. Gross rainfall, throughfall and stemflow monitoring

197 Atmospheric rainfall data was collected at Dinghushan Automatic Meteorological
198 Station from 2001–2022. Automatic meteorological systems were used to measure
199 atmospheric pressure (DPA501 gas-pressure meter), temperature (HMP45D sensor),
200 relative humidity (HMP45D sensor), rainfall (SM1-1 pluviometer), etc. Datalogger
201 (America Campbell, CR1000X) was used to control measurement sensors and store
202 meteorological data. The resolution of data recording was ± 0.2 mm with a time interval
203 of 10 min. The raw data comprised annual rainfall amounts, as well as single rainfall
204 events with throughfall and stemflow measurements.

205 Throughfall and stemflow were collected in all three forest types and
206 synchronously measured. Devices with cross-shaped collectors (1.25 m^2) attached to
207 reservoirs (1000 L) at the bottom were used to collect throughfall. Three throughfall
208 devices were randomly installed in each forest field (Fig. S1).

209 Half-shell plastic tubes were installed around tree trunks attached to reservoirs
210 (1000 L) at the bottom to collect stemflow. The ratio of volume (mL) to canopy area
211 (cm^2) is the stemflow (mm). A total of 24 trees ~~with six tree species~~ were selected to
212 measure stemflow volume (Table S2). In detail, four tree species were selected in the
213 broadleaf forest, including *Acmena acuminatissima* (Blume) Merr. et Perry (SF1),
214 *Cryptocarya chinensis* (Hance) Hemsl. (SF2), *Gironniera subaequalis* Planch. (SF3),
215 *Schima superba* Gardn. et Champ. (SF4), with 3 repetitions respectively. Three tree
216 species were selected in the mixed forest, including *Castanea henryi* (Skam) Rehd. et
217 Wils. (SF5), *Schima superba* Gardn. et Champ. (SF6), *Pinus massoniana* Lamb. (SF7),
218 with 3 repetitions respectively. In the pine forest, *Pinus massoniana* Lamb. (SF8) was

219 selected as the monitoring subject with 3 repetitions. ~~Growth indicators of the selected~~
220 ~~trees have been recorded every five years since 2000: tree height (m), DBH (cm), and~~
221 ~~crown area (CA, m²). Forest structures have been measured every five years since 2000:~~
222 ~~plant density (tree, shrub and herb), forest canopy coverage (%) and LAI.~~

224 2.3. Rainwater chemistry measurement

225 For the measurement of rainwater chemistry, rainwater samples were from 2000,
226 2010 and 2022 in Dinghushan area. The samples of open rainfall, throughfall and
227 stemflow were manually collected for every one-month period, respectively. The
228 samples of open rainfall and throughfall were collected with three repetitions,
229 respectively and stemflow with four repetitions in the broadleaf forest, three repetitions
230 in the mixed forest and three repetitions in the pine forest. In total, 792 rainwater
231 samples (108 open rainfall, 324 throughfall and 360 stemflow) were collected.

232 Rainwater samples were defrosted and filtered through 0.45 μm polypropylene
233 membranes. Concentrations of total nitrogen (TN) and total phosphorus (TP) were
234 measured using ultraviolet spectrophotometer (Lambda 25, Perkin-Elmer), and ion
235 potassium (K⁺) was measured using an inductively coupled plasma optical emission
236 spectrometer (Optima 2000, Perkin-Elmer), respectively. The origin data of TN, TP and
237 K⁺ were processed into annual flux and monthly values by weighted average method,

$$238 \quad C = \frac{\sum C_i * V_i}{\sum V_i} \quad (1)$$

239 where C_i and V_i are the concentrations of ions (mg L⁻¹) and water sample volume (L) in
240 each rainfall event, respectively.

242 2.4. Other measurement and statistical analysis

243 In the forests, plant density and canopy structure have been measured every five
244 years since 2000. 25 plots of 20 m × 20 m (A1-A25 plots) were built on a plot of 1hm²
245 to survey tree density (Fig. S1). Then, 25 plots of 5 m × 5 m (B1-B25 plots) were
246 randomly set on the A1-A25 plots to survey shrub density. Finally, 25 plots of 1 m × 1
247 m (C1-C25 plots) were randomly set on the B1-B25 plots to survey herb density. The
248 percentage of the surface area covered by plants to the total plot area is termed canopy
249 coverage (%). 25 observation plots (1 m × 1 m) were selected in the 1 hm² area of each
250 forest type. LAI (Leaf area index) was measured using a LAI-2200 plant canopy
251 analyzer with 90° view caps (Li-Cor Inc., USA). 10 observation points (distance about

10 m) were selected in the 1 hm² area of each forest type with 5 replications. Growth indicators of the selected trees have been recorded: tree height (m), diameter at breast height (DBH, cm), and crown area (CA, m²). Tree height was measured using laser range finder. Tape measure was used to measure the diameter of trees at a height of 1.3 m, namely DBH. CA: the laser rangefinder was used to measure the maximum diameter at the edge of the canopy, with multiple measurements at different points to ensure accuracy.

The differences in throughfall and stemflow among different forests were assessed using analysis of variance (ANOVA), followed by a Tukey test for multiple comparisons between means. Mann-Kendall (MK) test was used to analyze the variation trend of annual rainfall. All statistical procedures were conducted with $\alpha = 0.05$ threshold for significance, in the IBM SPSS statistics 22.0 software (IBM Inc.).

3. Results

3.1. ~~Open rainfall~~ Rainfall and temperature characteristics

Based on the 22 years rainfall dataset from the Dinghushan area, annual gross rainfall ranged between 1370.0 and 2361.1 mm (Fig. 1). ~~In detail, approximately 80%~~78.0% of gross rainfall appeared in the ~~rainy-wet~~ rainy-wet season (April–September). Result of M-K test showed that rainfall was in a significantly decreasing trend from 2001–2007 ($UF < 0, P < 0.05$), and shifted into a significantly increasing trend from 2012–2022 ($UF > 0, P < 0.05$). Moreover, 2008 and 2011 (the intersection of UF and UB) were the mutation time of rainfall trend ($P < 0.05$). Anomaly were revealed in the temporal variability (coefficient of variation, CV of 16.6%) in annual rainfall (Fig. 1a). ~~In details, some remarkable negative values in 2003–2005, 2007, 2011 and 2021 and positive values in 2006, 2008, 2015, 2018 and 2019 were found.~~ Anomaly varied at -426.4–476.8 mm and -258.0–471.4 mm in the ~~rainy-wet~~ rainy-wet season and dry season, respectively. By comparison, dry season experienced greater variation with CV of 40.4% than ~~rainy-wet~~ rainy-wet season with CV of 21.7%. Besides, annual raining days obviously tended to decrease over time from 2012 to 2021 (Fig. 1b). Based on five rainfall classifications, it was shown among 22 years that rainfall <10 mm account for about 68.5% of total raining days (2856), while rainfall >50 mm account for about 4.9%. Besides, annual temperature changed between 21.8 °C and 23.3 °C over 22 years. Result of M-K test showed statistically significant rising trend for temperature for 8 years out of 22 years

285 (UF > 0, P < 0.05). Moreover, 2005 and 2013–2014 were the mutation time of
286 temperature trend (P < 0.05).

288 3.2 Variability of throughfall

289 Rainfall redistribution (throughfall ~~+and~~ stemflow, ~~TS~~) among the three forests
290 all experienced differing magnitude during 22 years (Fig. 2). Annual throughfall were
291 concentrated between 954.2 mm and 2192.6 mm. Result of M-K test showed that
292 throughfall was in a significantly decreasing trend at first (UF < 0, P < 0.05) and then
293 shifted into an significantly increasing trend (UF > 0, P < 0.05) from 2001–2022,
294 similar with the trend of open rainfall. Differently, the mutation of throughfall trend
295 occurred in 2008, 2011 and 2021 in the broadleaf forest, 2008 and 2011 in the mixed
296 forest, 2006, 2008, 2011 and 2021 in the pine forest (P < 0.05). Anomalies of TS
297 ~~revealed that TS received below normal value similar with open rainfall.~~ For throughfall
298 ratio, it varied significantly both at the event and interannual scales (Fig. 3a, b and c).
299 The median of annual throughfall ratio in the broadleaf forest varied between 60% and
300 120% with CV of ~~13%~~16.4% from 2001–2022. The median of throughfall ratio in the
301 mixed pine and broadleaf forest varied between 80% and 110% with a CV of ~~10%~~9.7%.
302 The median of throughfall ratio in the pine forest varied between 59% and 110% with
303 a CV of ~~11%~~11.8%. Therefore, throughfall ratio was characterized by a relatively low
304 variability over annual-time scale (CV < ~~15%~~20%). Besides, some differences of
305 throughfall ratio were found among the three forest types based on rainfall
306 classifications (Fig. 3d). For rainfall events <-10 mm, throughfall ratio range in the
307 broadleaf forest was ~~35%~~30%–70%, while in the other two forest types it was ~~20%~~15%–
308 85% (Fig. 3d). The mean value of throughfall ratio was relatively small in the broadleaf
309 forest (53.9%), though no significant difference among the three forests (P > 0.05) were
310 detected. For rainfall events <50 mm, no significant difference of throughfall ratio
311 among the three forest types was found (P > 0.05). However, the average-median values
312 of throughfall ratio in the pine forest (90.0%) and the mixed forest (89.4%) were both
313 significantly larger than that in the broadleaf forest (83.7%) for rainfall events >50 mm.

314 CV values of throughfall based on all the rainfall event classifications were drawn
315 in the Fig. 4a. Results showed that median CV of throughfall in the pine forest (15.2%)
316 was lower than that for the broadleaf forest (21.7%) and for the mixed forest (26.3%)
317 for rainfall events <10 mm. For rainfall events >10 mm, small differences of median
318 CV among the three forest types were shown. Meanwhile, CV values decreased with

319 the increasing rainfall events, eventually falling to 3.5%–4.3%. Besides, CV values of
320 throughfall based on interannual scale were drawn in the Fig. 5a, b and c. Annual CV
321 values among different forest types showed different fluctuations over time. The
322 medians of CV in annual, rainy-wet and dry seasons presented different order in
323 different years. According to linear fitting, significant negative correlations were found
324 in the median of CV_{TF} in the mixed forest over time ($r = 0.63$, $P < 0.01$). In addition,
325 fitting result of in total 740 rainfall events in 22 years showed that CV values of
326 throughfall significantly decreased with increasing gross rainfall (Fig. S1S2).

3.3 Variability of stemflow

329 Annual stemflow was concentrated between 9.0 and 119.7 mm over 22 years (Fig.
330 2). More stemflow were collected in the broadleaf forest and mixed forest than in the
331 pine forest. Result of M-K test showed that stemflow of both broadleaf forest and mixed
332 forest were in a decreasing trend at first ($UF < 0$, $P < 0.05$) and then shifted into an
333 increasing trend ($UF > 0$, $P < 0.05$), different from continuously increasing trend of
334 pine forest ($UF > 0$). The mutation of stemflow trend occurred in 2008 in the broadleaf
335 forest, 2011 in the mixed forest, 2006, 2012 and 2015 in the pine forest ($P < 0.05$).
336 Stemflow ratio changed significantly both at the event and interannual scales (Fig. 3a,
337 b and c). Among 22 years, the median of annual stemflow ratio in the broadleaf forest
338 varied between 1.3% and 5.4% with a CV of 56.2%. The stemflow ratio of mixed forest
339 varied between 1.5% and 4.4% with a CV of 38.6%. In the pine forest, it varied between
340 0.3% and 1% with a CV of 50.9%. This indicated that the stemflow ratio was
341 characterized by an extremely high variability over time. Same to the seasonal
342 throughfall ratio, the medians of stemflow ratio in annual, rainy-wet and dry seasons
343 presented different orders in different years. Besides, the stemflow ratio significantly
344 changed among tree species and among rainfall classifications (Fig. 3e). By comparison,
345 stemflow ratios of the SF1 and SF2 trees in the broadleaf forest were both higher in all
346 the tree species for the rainfall events < 50 mm. However, for strong events (> 50 mm),
347 the stemflow ratio of the SF5 tree in the mixed forest was highest for all tree species,
348 followed by the trees in the broadleaf forest. For all the rainfall events, the stemflow
349 ratio of SF7 in the mixed forest and SF8 in the pine forest were both lower than that for
350 other tree species.

351 CV values of stemflow based on rainfall event classifications were drawn in the
352 Fig. 4b. By comparison, stemflow varied more than those of throughfall across rainfall

353 events, with CV_{SF} values of 25%–130%. Median CV of stemflow in the pine forest was
354 always lower (45%–68%) than that for the other two forest types (56%–120%). CV
355 values of stemflow based on interannual scale changed over time among different forest
356 types (Fig. 5d, e and f). The medians of CV_{SF} in annual, ~~rainy-wet~~ and dry seasons
357 presented different order in different years. By comparison, CV_{SF} was always greater
358 than CV_{TF} , and interannual fluctuation of CV_{SF} was also stronger than CV_{TF} . According
359 to linear fitting, significant negative correlations were found in the median of CV_{SF} in
360 the broadleaf forest over time ($r = 0.73, P < 0.001$). In addition, fitting result of in total
361 740 rainfall events in 22 years showed that CV values of stemflow both significantly
362 decreased with increasing gross rainfall (Fig. ~~S1~~S2).

363

364 3.4. Rainwater chemistry

365 Rainwater (open rainfall, throughfall and stemflow) chemical properties (TN, TP
366 and K^+ concentration) were measured in the three forest types, respectively. All of TN,
367 TP and K^+ values presented in order stemflow > throughfall > open rainfall (Fig. 6a, b
368 and c). However, changes of TN, TP and K^+ were different for the three forest types
369 among 2000, 2010 and 2022. For instance, in 2000 and 2010, TN values of throughfall
370 and stemflow decreased for both in order of pine forest > mixed forest > broadleaf forest,
371 while no such result could be confirmed in 2022. Similarly, TP values of throughfall in
372 broadleaf forest was 1.3 times higher than that in pine forest in 2022, while TP values
373 in pine forest was 6.8 times ~~s~~ than that in broadleaf forest in 2000. K^+ values of stemflow
374 in 2010 (6.76 mg L⁻¹) and 2022 (6.22 mg L⁻¹) were higher for broadleaf forest than
375 those for pine forest (3.76 mg L⁻¹ and 2.46 mg L⁻¹), which was different from that in
376 2022.

377 TN, TP and K^+ fluxes of stemflow were < 10 kg ha⁻¹ a⁻¹, 0.2 kg ha⁻¹ a⁻¹, 6 kg ha⁻¹
378 a⁻¹, respectively, all lower than those of throughfall and open rainfall (Fig. 7d, e and f).
379 In the 2000, 2010 and 2022, TN flux (39.4–87.4 kg ha⁻¹ a⁻¹) was 1.2–1.8 times greater
380 than that of open rainfall, 3.3–28.0 times greater than that of stemflow. TP flux (1.1–
381 2.7 kg ha⁻¹ a⁻¹) was 1.0–2.3 times greater than that of open rainfall, 8.7–31.4 times
382 greater than that of stemflow. K^+ flux (21.5–59.2 kg ha⁻¹ a⁻¹) was 2.2–8.1 times greater
383 than that of open rainfall, 2.2–26.8 times greater than that of stemflow. In addition, TN,
384 TP and K^+ fluxes of stemflow increased with succession from primary to climax,
385 namely pine forest < mixed forest < broadleaf forest. Different from this, differences in

386 chemistry fluxes of throughfall was not found among different forests, neither among
387 different periods.

388 Besides, monthly chemistry concentrations in rainfall, throughfall and stemflow
389 showed distinct changes (Fig. 7). Monthly TN, TP and K^+ concentrations of rainfall
390 were always lower than those of stemflow for all trees. Monthly TN, TP and K^+ of
391 stemflow in the dry season were generally higher than in the ~~rainy-wet~~ season. High
392 monthly TN concentrations of stemflow with SF6 of mixed forest and SF8 of pine forest
393 were found, especially in dry season with maximum TN concentrations of 27.59 mg L⁻¹
394 at SF6 and 19.94 mg L⁻¹ at SF8, respectively. Differently, high monthly K^+
395 concentration of stemflow at SF4 in broadleaf forest was found, with in dry season
396 maximum K^+ concentration of 25.17 mg L⁻¹.

397

398 **4. Discussion**

399 *4.1. Open rainfall partitioned to throughfall and stemflow*

400 Studies in forests have confirmed that throughfall volume increased with
401 increasing gross rainfall at event scale, accounting for 60%–80% of gross rainfall (Ji et
402 al., 2023; André et al., 2011; Carlyle-Moses, 2004). ~~This study, with 22 years of data,~~
403 ~~showed that annual rainfall changed over long-time scale and for different rainfall~~
404 ~~classifications (Fig. 1), which can directly affect annual throughfall.~~ Throughfall ratio
405 changed over time and showed different fluctuations among different forests (Fig. 3).
406 During light rainfall events with rainfall amounts <10 mm, a low proportion of
407 raindrops would reach the ground as throughfall, as the tree canopy intercepts almost
408 all the incoming raindrops. Specifically, high canopy coverage in broadleaf forest can
409 reinforce raindrop intercept (Brasil et al., 2018; Ponette-González et al., 2010),
410 consequently generating lower throughfall ratio than those in the mixed forest and pine
411 forest (Fig. 3). During moderate rainfall events (10–50 mm), given that the intercept
412 effect of the wetting tree canopy was weakened (Shinohara et al., 2015), throughfall
413 ratio was in a high and steady state. As the gross rainfall increases further (>50 mm),
414 significant differences of throughfall ratio were found among the three forests.
415 Throughfall ratio was significantly lower in the broadleaf forest than those in the other
416 two forests. Likewise, such differences due to rainfall event class also appeared in other
417 forest studies with stands such as beech, pine in monocultures and mixed pine-beech
418 (Blume et al., 2022). Influenced by forest stand characteristics, throughfall therefore

419 indicated different forest water budget.

420 Stemflow ~~ratio~~ of forests were variably controlled by tree species, on average
421 accounting for about <10% of gross rainfall, even lower (<1%) (Sun et al., 2018; André
422 et al., 2008; Crockford and Richardson, 1990). In our study site, the lowest stemflow
423 (<1%) was collected in the pine forest, though weakly increasing with rainfall
424 classifications (Fig. 3). Stemflow ratio in broadleaf forest was maintained at 5%–10%
425 without the effect of rainfall amount seemingly. In detail, stemflow ratio of pine forest
426 (SF8) was significantly lower than those of broadleaf forest (SF1~4). And in the mixed
427 forest, broad-leaved trees (SF5 and SF 6) have larger stemflow than pine tree (SF7).
428 However, for some rainfall events, extraordinary low proportion of stemflow in the
429 broadleaf forest and extraordinary high proportion in the pine forest were caught. This
430 implied the key role of rainfall conditions (e.g., intensity, duration) and tree species with
431 tree traits (e.g., branch angle), consistent with reported studies e.g., in evergreen forest
432 (Chen et al., 2019; Bruijnzeel et al., 2011) and pine forest ([Pinos et al., 2021](#); Crockford
433 and Richardson, 1990). Moreover, ANOVA showed significant differences of stemflow
434 ratio among tree species and rainfall classifications ($P < 0.001$) (Table 1). This indicated
435 that rainfall and tree species simultaneously affect stemflow. Branch inclination angle,
436 canopy cover, tree height and DBH of tree species proved to be key factors in stemflow
437 yield (Levia et al., 2015).

438 Throughfall and stemflow were generally enriched in chemical concentration
439 compared with open rainfall due to leachable canopy/stem ion pools (Jiang et al., 2021;
440 Van Stan et al., 2017; Zimmermann et al., 2007). In our study, the concentration of K^+
441 in stemflow was 16 times higher than that in open rainfall and in throughfall reached
442 up to 11 times higher than open rainfall (Fig. 6). Similar results were also found in
443 artificial plantation (*Acacia mangium* and *Dimocarpus longan*) of South China (Shen
444 et al., 2013), in Oriental beech (*Fagus orientalis* Lipsky) trees in Northern Iran (Moslehi
445 et al., 2019), indicating strong K^+ leaching from canopy. Even so, throughfall was
446 generally characterized with high fluxes compared to open rainfall followed by
447 stemflow, it thus is the largest contributor to wet deposition. Meanwhile, TN flux of
448 throughfall was greatest in the pine forest in 2010, TP flux of throughfall was greatest
449 in the broadleaf forest in 2000, and K^+ flux of throughfall was greatest in the mixed
450 forest in 2010. It should be noted that the differences of rainwater chemistry shifted
451 over time among the three forests. Accordingly, throughfall and stemflow via canopy
452 and stem input soil is a significant contributor, and its long-term effect on ecosystems

453 needs more attention (Fan et al., 2021). After all, atmospheric wet deposition provides
454 nutrient requirement for ecosystems, but also imposes a considerable burden on the
455 ecosystems in general. For instance, N enrichment and P limitation have proven to have
456 different effect on soil carbon sequestration, microbial community composition and
457 forest productivity, especially in tropical and subtropical forest ecosystems with highly
458 weathered soils (Zheng et al., 2022; Li et al., 2016; Huang et al., 2012). Besides,
459 throughfall and stemflow was mainly characterized by low chemical concentrations in
460 the ~~rainy-wet~~ season and high concentrations in the dry season. Primary reasons for
461 seasonal rainwater chemistry may be attributable to moisture source associated with
462 frontal weather systems and gradually depleting effect with increasing rainfall amount
463 (Dunkerley, 2014; Germer et al., 2007). The present study in subtropical forests and
464 previous studies in tropical forests and European temperate forests all exhibited variable
465 rainwater chemistry in throughfall and stemflow, both spatially and temporally
466 (Zimmermann et al., 2007; Staelens et al., 2006; Seiler and Matzner, 1995). In fact, the
467 chemical concentration of rainfall redistribution was also affected profoundly by
468 canopy and stem parameters of tree species (Tonello et al., ~~2021a~~2021b; Chen et al.,
469 2019). In our study, some differences of TN, TP and K⁺ were also found among
470 SF1~SF8 due to tree-species specific effect (Legout et al., 2016; De Schrijver et al.,
471 2007).

472

473 4.2. Long-term changes of rainfall in forests

474 Rainfall regimes induce divergent spatially hydrological changes (Wu et al., 2024).
475 Likewise, our study found that throughfall of forests experienced a decreasing followed
476 by an increasing from 2001–2022, similar with the trend of open rainfall, and stemflow
477 showed characteristic trends in different forests especially in the pine forest (Fig. 1).
478 This suggested that ~~At the long-time scale of 22 years,~~ the complexity of forest structure
479 and rainfall amount and their change exacerbated the spatio-temporal variability of
480 throughfall and stemflow. Firstly, interannual variability of forest structure (e.g., canopy
481 coverage, leaf area index) and tree parameters (e.g., height, DBH and CA) made
482 throughfall and stemflow distribution uncertain (Yue et al., 2021). From 2001 to 2022,
483 changes in forest structure were confirmed in all three forests, such as changes in plant
484 density, canopy coverage and LAI (Fig. 8). Throughfall ratio and stemflow ratio in the
485 succession forest systems all varied over time accordingly. Similarly, driven by forest
486 structure (e.g., tree density, species dominance), a six-year dataset from the Brazilian

487 Atlantic Forest showed that the spatial variability of throughfall over time was less
488 stable (Rodrigues et al., 2022). Besides, the variation of stemflow (CV_{SF}) was obviously
489 larger than that of throughfall (CV_{TF}) (Fig. 4), which probably was attributed to the
490 differences of tree species in stemflow (Fig. 3). For a forest succession, a 17 years'
491 study showed that the shift from monoculture Japanese red pine to mixture of red pine,
492 evergreen oak and theaceous tree made stemflow significantly increasing (Iida et al.,
493 2005). Likewise, for the forest succession in Dinghushan area, stemflow ratio in
494 broadleaf forest and mixed forest were both higher than that in tree-monospecific pine
495 forest. High plant density (tree and shrub) and LAI in broadleaf forest and mixed forest
496 conduce to rainwater interception of multi-canopy trees through more leaves and angled
497 branches, which potentially enhanced stemflow (Fig. 8). Indeed, some differences of
498 rainfall redistribution appeared in multi-layered vegetative structure. An experiment on
499 vegetation communities with a complex multi-layered structure found that interception
500 loss from shrubs was two-times higher than from trees, and smaller trees generated
501 stemflow more efficiently than the higher ones (Exler and Moore, 2022). Based on the
502 22 years' data from forest community survey in our study site, forest canopy parameters
503 (e.g., coverage and LAI) of trees and shrubs showed variation over time from 2001 to
504 2022 (Fig. 8). In the broadleaf forest, plant density of trees and canopy coverage of
505 shrubs showed a slight increment compared to the other two forests, though LAI was
506 decreasing. During this period, interannual throughfall ratio and stemflow ratio showed
507 significantly change over time (Fig. 3), implying the role of interannual variation of
508 forest structure in rainfall redistribution process.

509 Secondly, ongoing rainfall changes with different magnitude favor the different
510 levels of rainfall redistribution over time (Lian et al., 2022). At event scale, throughfall
511 and stemflow proportions of forests were both low with rainfall events <10 mm. The
512 variations of throughfall and stemflow were both larger for gross rainfall <10 mm than
513 events >10 mm. Rainfall threshold associated with the canopy interception capacity had
514 impact on throughfall and stemflow generation (Zabret et al., 2018; André et al., 2008;
515 Durocher, 1990). After the raindrop capacity of the canopy reached its peak, throughfall
516 and stemflow were documented to match the gross rainfall. Therefore, relatively low
517 proportions and high spatial variability appeared before rainfall threshold, and after that,
518 relatively high proportions and low variability until a stable level were observed in the
519 three forests. Moreover, at interannual scale, the raining days in different magnitudes
520 presented obvious fluctuation over 22 years (Fig. 1). This fluctuation of raining days

521 and its magnitude distribution potentially regulated the long-term changes of open
522 rainfall partitioned to interception loss, throughfall and stemflow. Consequently,
523 throughfall and stemflow, influenced by the comprehensive effect of rainfall regimes
524 and forest structures, presented spatiotemporal variability at different level (Fig. 3–6).
525 From a long-term perspective, changing in rainfall redistribution potentially makes
526 forest water and biogeochemistry budget more complex. Further knowledge of the
527 long-term accumulative effect of rainfall redistribution on forest water and chemistry
528 (e.g., soil and plant) is needed in the future.

529 Throughfall and stemflow are part of rainfall and are key player in the water cycle
530 process. Based on the connection of the water cycle to precipitation and temperature
531 and under the background of climate change, frequency of extreme events (heavy
532 rainfall, droughts) needs to be anticipated in the effect on rainfall redistribution and
533 solute transport within forests, which in turn may affect the water cycle and
534 biogeochemical cycles (Blume et al., 2022). In this study, it should be noted that the
535 2008 rainfall data can be used as an example under extreme event. In 2008, extreme
536 weather events occurred in South China. Freezing events occurred in the dry season,
537 continuous heavy rain and typhoon events occurred in the wet season. Gross rainfall
538 was larger than other years, with the annual rainfall of 2361.1 mm (22-year average
539 annual rainfall of 1848.6 mm) (Fig. 1). At the same time, a total of 26 throughfall events
540 were collected in 2008. According to the M-K test, the throughfall and stemflow trend
541 of different forests presented different degree of disturbance under the background of
542 mutation of open rainfall (Fig. 2). In this process, the driving effect of forest structure
543 and rainfall on throughfall and stemflow mutation is synchronous. More data and
544 modeling are needed to support the relevant study about effect of climate change on
545 rainfall redistribution in the future.

546

547 **5. Conclusion**

548 The current study investigated long-term changing characteristic of rainfall
549 redistribution along a subtropical forest succession sequence with: pine forest (PF),
550 mixed pine and broadleaf forest (MF) and monsoon evergreen broadleaf forest (BF).
551 Firstly, in the valid 740 rainfall events throughfall ratio showed in order $BF < MF < PF$,
552 and stemflow ratio showed in order $BF > MF > PF$. The variation of stemflow was
553 higher ($CV > 50\%$) than that of throughfall ($CV < 25\%$). Secondly, throughfall and
554 stemflow of forests experienced a decreasing followed by an increasing from 2001–

555 2022 (except stemflow of the pine forest), similar with the trend of open rainfall. Driven
556 by rainfall and forest factors, interannual variability of both throughfall and stemflow
557 in the broadleaf forest were greater than those in the mixed forest and pine forest, which
558 was different from that of annual open rainfall. 22 years' monitored data showed that
559 throughfall ratio widely changed between 30% and 90%, and stemflow ratio changed
560 between 0.1% and 10%. Annual gross rainfall considerably changed over time, which
561 directly induced the variable accumulation of annual throughfall and annual stemflow.

562 For rainwater chemistry, differences of the clement flux in throughfall and
563 stemflow among the three forest types were confirmed based on data from 2001, 2010
564 and 2022. On average, TN and TP fluxes of throughfall presented in order BF < MF <
565 PF, while K⁺ flux of throughfall presented in order BF > MF > PF. Over time, rainwater
566 chemical concentrations were lower in the wet season than that in the dry season. Given
567 the smaller proportion of open rainfall, stemflow chemical fluxes varied less among
568 forest types and/or over time, though tree species exactly contribute to differences in
569 stemflow chemistry. Nevertheless, its funnel effect on soil and plant over time still
570 deserves more attention in the future. ~~stemflow was characterized with high TN, TP~~
571 ~~and K⁺ concentrations compared to throughfall followed by open rainfall. Rainwater~~
572 ~~chemical concentrations were lower in the rainy season than that in the dry season.~~
573 ~~However, throughfall, characterized with high fluxes compared to open rainfall~~
574 ~~followed by stemflow, is the largest contributor to wet deposition. Additionally,~~
575 ~~differences of the rainwater chemical concentrations among the three forest types were~~
576 ~~confirmed over time based on data from 2001, 2010 and 2022. On average, TN and TP~~
577 ~~fluxes of throughfall presented in order BF < MF < PF, while K⁺ flux of throughfall~~
578 ~~presented in order BF > MF > PF.~~

579 The above results indicate that the water volume and chemistry in rainfall
580 redistribution process under forest represented not exactly the same trend as open
581 rainfall are variable over time, and throughfall and stemflow depend on the effect of
582 rainfall and forest factors. This study thus provided insight into the rainfall
583 redistribution process by linking the long-term change of rainfall pattern with a
584 subtropical forest succession sequence.

585
586
587 *Code and data availability.* The data used to derive to the conclusions of the present
588 study are freely accessible. All the data were obtained from the CNERN dataset

589 (<http://dhf.cern.ac.cn/meta/metaData>).

590

591 *Author contributions.* WJZ: conceptualization, investigation, data analysis, writing,
592 visualization. TS and SS: reviewing, supervision. QMZ and CGW: resources, data
593 curation, WLH: reviewing, JXL and XX: reviewing, funding acquisition, supervision

594

595 *Competing interests.* The authors declare that they have no conflict of interest.

596

597 *Disclaimer.* Publisher's note: Copernicus Publications remains neutral with regard to
598 jurisdictional claims made in the text, published maps, institutional affiliations, or any
599 other geographical representation in this paper. While Copernicus Publications makes
600 every effort to include appropriate place names, the final responsibility lies with the
601 authors.

602

603 *Acknowledgements.* Wanjun Zhang would like to acknowledge the financial support
604 from the CSC Fellowship.

605

606 *Financial support.* This research has been supported by The Key-Area Research and
607 Development Program of Guangdong Province (Grant No. 2022B1111230001), the
608 National Natural Science Foundation of China (Grant Nos. 42207158 and 32101342)
609 and the China Postdoctoral Science Foundation (Grant Nos. 2021M703259, 2021
610 M703260, 2021M693220).

611

612

613 **References**

614 André, F., Jonard, M., Jonard, F., Ponette, Q., 2011. Spatial and temporal patterns of throughfall volume
615 in a deciduous mixed-species stand. *J. Hydrol.* 400(1–2), 244–254.
616 <https://doi.org/10.1016/j.jhydrol.2011.01.037>

617 André, F., Jonard, M., Ponette, Q. (2008). Influence of species and rain event characteristics on stemflow
618 volume in a temperate mixed oak–beech stand. *Hydrol. Process.* 22(22), 4455–4466.
619 <https://doi.org/10.1002/hyp.7048>

620 Blume, T., Schneider, L., Güntner, A., 2022. Comparative analysis of throughfall observations in six
621 different forest stands: Influence of seasons, rainfall-and stand characteristics. *Hydrol. Process.*
622 36(3), e14461. <https://doi.org/10.1002/hyp.14461>

623 Borghetti, M., Gentilesca, T., Leonardi, S., Van Noije, T., Rita, A., 2017. Long-term temporal

624 relationships between environmental conditions and xylem functional traits: a meta-analysis across
625 a range of woody species along climatic and nitrogen deposition gradients. *Tree Physiol.* 37(1), 4-
626 17.

627 Brasil, J.B., Andrade, E.M.d., Palácio, H.A.d.Q., Medeiros, P.H.A., Santos, J.C.N.d., 2018.
628 Characteristics of precipitation and the process of interception in a seasonally dry tropical forest. *J.*
629 *Hydrol-Reg. Stud.* 19, 307–317. <https://doi.org/10.1016/j.ejrh.2018.10.006>

630 Brauman, K.A., Freyberg, D.L., Daily, G.C., 2010. Forest structure influences on rainfall partitioning
631 and cloud interception: A comparison of native forest sites in Kona, Hawai'i. *Agric. For. Meteorol.*
632 150(2), 265–275. <https://doi.org/10.1016/j.agrformet.2009.11.011>

633 Bruijnzeel, L.A., Mulligan, M., Scatena, F.N., 2011. Hydrometeorology of tropical montane cloud forests:
634 emerging patterns. *Hydrol. Process.* 25(3), 465–498. <https://doi.org/10.1002/hyp.7974>

635 Carlyle-Moses, D.E., Laureano, J.F., Price, A.G., 2004. Throughfall and throughfall spatial variability in
636 Madrean oak forest communities of northeastern Mexico. *J. Hydrol.* 297(1–4), 124–135.
637 <https://doi.org/10.1016/j.jhydrol.2004.04.007>

638 Chen, S., Cao, R., Yoshitake, S., Ohtsuka, T., 2019. Stemflow hydrology and DOM flux in relation to
639 tree size and rainfall event characteristics. *Agric. For. Meteorol.* 279, 107753.
640 <https://doi.org/10.1016/j.agrformet.2019.107753>

641 Crockford, R.H., Richardson, D.P., 1990. Partitioning of rainfall in a eucalypt forest and pine plantation
642 in southeastern Australia: II Stemflow and factors affecting stemflow in a dry sclerophyll eucalypt
643 forest and a *Pinus radiata* plantation. *Hydrol. Process.* 4(2), 145–155.
644 <https://doi.org/10.1002/hyp.3360040205>

645 De Schrijver, A., Geudens, G., Augusto, L., Staelens, J., Mertens, J., Wuyts, K., Gielis, L., Verheyen, K.
646 (2007). The effect of forest type on throughfall deposition and seepage flux: a review. *Oecologia*,
647 153, 663-674. <https://doi.org/10.1007/s00442-007-0776-1>

648 Dunkerley, D., 2014. Stemflow on the woody parts of plants: dependence on rainfall intensity and event
649 profile from laboratory simulations. *Hydrol. Process.* 28(22), 5469–5482.
650 <https://doi.org/10.1002/hyp.10050>

651 Durocher, M.G., 1990. Monitoring spatial variability of forest interception. *Hydrol. Process.* 4(3), 215–
652 229. <https://doi.org/10.1002/hyp.3360040303>

653 Exler, J.L., Moore, R.D., 2022. Quantifying throughfall, stemflow and interception loss in five vegetation
654 communities in a maritime raised bog. *Agric. For. Meteorol.* 327, 109202.
655 <https://doi.org/10.1016/j.agrformet.2022.109202>

656 Fan, Y.X., Lu, S.X., He, M., Yang, L.M., Hu, W.F., Yang, Z.J., Liu, X.F., Hui, D.F., Guo, J.F., Yang, Y.S.,
657 2021. Long-term throughfall exclusion decreases soil organic phosphorus associated with reduced
658 plant roots and soil microbial biomass in a subtropical forest. *Geoderma*, 404, 115309.
659 <https://doi.org/10.1016/j.geoderma.2021.115309>

660 Germer, S., Elsenbeer, H., Moraes, J.M., 2006. Throughfall and temporal trends of rainfall redistribution
661 in an open tropical rainforest, south-western Amazonia (Rondônia, Brazil). *Hydrol. Earth Syst. Sci.*
662 10(3), 383–393. <https://doi.org/10.5194/hess-10-383-2006>

663 Germer, S., Neill, C., Krusche, A.V., Neto, S.C.G., Elsenbeer, H., 2007. Seasonal and within-event

664 dynamics of rainfall and throughfall chemistry in an open tropical rainforest in Rondônia, Brazil.
665 Biogeochemistry, 86, 155–174. <https://doi.org/10.1007/s10533-007-9152-9>

666 Germer, S., Werther, L., Elsenbeer, H., 2010. Have we underestimated stemflow? Lessons from an open
667 tropical rainforest. *J. Hydrol.* 395(3-4), 169–179. <https://doi.org/10.1016/j.jhydrol.2010.10.022>

668 Goebes, P., Bruelheide, H., Härdtle, W., Kröber, W., Kühn, P., Li, Y., Seitz, S., von Oheimb, G., Scholten,
669 T., 2015. Species-specific effects on throughfall kinetic energy in subtropical forest plantations are
670 related to leaf traits and tree architecture. *PLoS one*, 10(6), e0128084.
671 <https://doi.org/10.1371/journal.pone.0128084>

672 Grunicke, S., Queck, R., Bernhofer, C., 2020. Long-term investigation of forest canopy rainfall
673 interception for a spruce stand. *Agric. For. Meteorol.* 292, 108125.
674 <https://doi.org/10.1016/j.agrformet.2020.108125>

675 Grossiord, C., Sevanto, S., Dawson, T. E., Adams, H.D., Collins, A.D., Dickman, L.T., Newman B.D.,
676 Stockton, E.A., McDowell, N.G. (2017). Warming combined with more extreme precipitation
677 regimes modifies the water sources used by trees. *New Phytol.* 213(2), 584–596.
678 <https://doi.org/10.1111/nph.14192>

679 Huang, W.J., Zhou, G.Y., Liu, J.X., 2012. Nitrogen and phosphorus status and their influence on
680 aboveground production under increasing nitrogen deposition in three successional forests. *Acta*
681 *Oecologica*, 44, 20–27. <https://doi.org/10.1016/j.actao.2011.06.005>

682 Iida, S.I., Tanaka, T., Sugita, M., 2005. Change of interception process due to the succession from
683 Japanese red pine to evergreen oak. *J. Hydrol.* 315(1–4), 154–166.
684 <https://doi.org/10.1016/j.jhydrol.2005.03.024>

685 Jackson, N.A., 2000. Measured and modelled rainfall interception loss from an agroforestry system in
686 Kenya. *Agric. For. Meteorol.* 100, 323–336. [https://doi.org/10.1016/S0168-1923\(99\)00145-8](https://doi.org/10.1016/S0168-1923(99)00145-8)

687 Ji, S.Y., Omar, S.I., Zhang, S.B, Wang, T.F, Chen, C.F, Zhang, W.J., 2022. Comprehensive evaluation of
688 throughfall erosion in the banana plantation. *Earth Surf. Proc. Land.*, 47(12), 2941–2949.
689 <https://doi.org/10.1002/esp.5435>

690 Jiang, Z.Y., Zhi, Q.Y., Van Stan, J.T., Zhang, S.Y., Xiao, Y.H., Chen, X.Y., Wu, H.W., 2021. Rainfall
691 partitioning and associated chemical alteration in three subtropical urban tree species. *J. Hydrol.*
692 603, 127109. <https://doi.org/10.1016/j.jhydrol.2021.127109>

693 Junior, J.J., Mello, C.R., Owens, P.R., Mello, J.M., Curi, N., Alves, G.J., 2017. Time-stability of soil
694 water content (SWC) in an Atlantic Forest-Latosol site. *Geoderma*, 288, 64–78.
695 <https://doi.org/10.1016/j.geoderma.2016.10.034>

696 Keim, R.F., Tromp-van Meerveld, H.J., McDonnell, J.J., 2006. A virtual experiment on the effects of
697 evaporation and intensity smoothing by canopy interception on subsurface stormflow generation. *J.*
698 *Hydrol.* 327(3–4), 352–364. <https://doi.org/10.1016/j.jhydrol.2005.11.024>

699 Klos, P.Z., Chain-Guadarrama, A., Link, T.E., Finegan, B., Vierling, L.A., Chazdon, R., 2014.
700 Throughfall heterogeneity in tropical forested landscapes as a focal mechanism for deep percolation.
701 *J. Hydrol.* 519, 2180–2188. <https://doi.org/10.1016/j.jhydrol.2014.10.004>

702 Kotteck, M., Grieser, J., Beck, C., Rudolf, B., Rubel, F., 2006. World map of the Köppen-Geiger climate
703 classification updated. *Meteorologische Zeitschrift*, 15(3), 259–263. [22](https://doi.org/10.1127/0941-</p>
</div>
<div data-bbox=)

704 2948/2006/0130

705 Lacombe, G., Valentin, C., Sounyafong, P., De Rouw, A., Souleuth, B., Silvera, N., Pierret, A.,
706 Sengtaheuanghong, O., Ribolzi, O., 2018. Linking crop structure, throughfall, soil surface
707 conditions, runoff and soil detachment: 10 land uses analyzed in Northern Laos. *Sci. Total Environ.*
708 616, 1330–1338. <https://doi.org/10.1016/j.scitotenv.2017.10.185>

709 Legout, A., van Der Heijden, G., Jaffrain, J., Boudot, J. P., Ranger, J., 2016. Tree species effects on
710 solution chemistry and major element fluxes: A case study in the Morvan (Breuil, France). *Forest*
711 *Ecol Manag.* 378, 244–258. <https://doi.org/10.1016/j.foreco.2016.07.003>

712 Leuzinger, S., Körner, C., 2010. Rainfall distribution is the main driver of runoff under future CO₂-
713 concentration in a temperate deciduous forest. *Global Change Biol.* 16(1), 246–254.
714 <https://doi.org/10.1111/j.1365-2486.2009.01937.x>

715 Levia, D. F., Nanko, K., Amasaki, H., Giambelluca, T. W., Hotta, N., Iida, S. I., Mudd, R.G., Nullet, M.A.,
716 Sakai, N., Shinori, Y., Sun X.C., Suzuki, M., Tanaka, N., Tantasirin, C., Yamada, K., 2019.
717 Throughfall partitioning by trees. *Hydrol. Process.* 33(12), 1698–1708.
718 <https://doi.org/10.1002/hyp.13432>

719 Levia, D.F., Germer, S., 2015. A review of stemflow generation dynamics and stemflow-environment
720 interactions in forests and shrublands. *Rev. Geophys.* 53(3), 673–714.
721 <https://doi.org/10.1002/2015RG000479>

722 Levia Jr, D.F., Frost, E.E., 2006. Variability of throughfall volume and solute inputs in wooded
723 ecosystems. *Prog. Phys. Geog.* 30(5), 605–632. <https://doi.org/10.1177/0309133306071145>

724 Li, Y., Niu, S.L, Yu, G.R., 2016. Aggravated phosphorus limitation on biomass production under
725 increasing nitrogen loading: a meta-analysis. *Global Change Biol.* 22(2), 934–943.
726 <https://doi.org/10.1111/gcb.13125>

727 Lian, X., Zhao, W.L., Gentine, P., 2022. Recent global decline in rainfall interception loss due to altered
728 rainfall regimes. *Nat. Commun.* 13(1), 7642. <https://doi.org/10.1038/s41467-022-35414-y>

729 Liu, J.Q., Liu, W.J., Li, W.X., Zeng, H.H., 2019. How does a rubber plantation affect the spatial variability
730 and temporal stability of throughfall? *Hydrol. Res.* 50(1), 60–74.
731 <https://doi.org/10.2166/nh.2018.028>

732 Livesley, S.J., Baudinette, B., Glover, D., 2014. Rainfall interception and stem flow by eucalypt street
733 trees – The impacts of canopy density and bark type. *Urban For. Urban Gree.* 13(1), 192–197.
734 <https://doi.org/10.1016/j.ufug.2013.09.001>

735 Llorens, P., Domingo, F., 2007. Rainfall partitioning by vegetation under Mediterranean conditions. A
736 review of studies in Europe. *J. Hydrol.* 335(1–2), 37–54.
737 <https://doi.org/10.1016/j.jhydrol.2006.10.032>

738 Llorens, P., Latron, J., Carlyle-Moses, D.E., Nätthe, K., Chang, J.L., Nanko, K., Lida, S., Levia, D.F.,
739 2022. Stemflow infiltration areas into forest soils around American beech (*Fagus grandifolia* Ehrh.)
740 trees. *Ecohydrology* 15(2), e2369. <https://doi.org/10.1002/eco.2369>

741 Loustau, D., Berbigier, P., Granier, A., 1992. Interception loss, throughfall and stemflow in a maritime
742 pine stand. II. An application of Gash's analytical model of interception. *J. Hydrol.* 138(3–4), 469–
743 485. [https://doi.org/10.1016/0022-1694\(92\)90131-E](https://doi.org/10.1016/0022-1694(92)90131-E)

- 744 Marin, C.T., Bouten, W., Sevink, J., 2000. Gross rainfall and its partitioning into throughfall, stemflow
745 and evaporation of intercepted water in four forest ecosystems in western Amazonia. *J. Hydrol.*
746 237(1–2), 40–57. [https://doi.org/10.1016/S0022-1694\(00\)00301-2](https://doi.org/10.1016/S0022-1694(00)00301-2)
- 747 Moslehi, M., Habashi, H., Khormali, F., Ahmadi, A., Brunner, I., Zimmermann, S., 2019. Base cation
748 dynamics in rainfall, throughfall, litterflow and soil solution under Oriental beech (*Fagus orientalis*
749 Lipsky) trees in northern Iran. *Ann. Forest Sci.* 76(2), 1–12. [https://doi.org/10.1007/s13595-019-](https://doi.org/10.1007/s13595-019-0837-8)
750 0837-8
- 751 Muzyło, A., Llorens, P., Domingo, F., 2012. Rainfall partitioning in a deciduous forest plot in leafed and
752 leafless periods. *Ecohydrology*, 5(6), 759–767. <https://doi.org/10.1002/eco.266>
- 753 Nanko, K., Hotta, N., Suzuki, M., 2006. Evaluating the influence of canopy species and meteorological
754 factors on throughfall drop size distribution. *J. Hydrol.* 329(3–4), 422–431.
755 <https://doi.org/10.1016/j.jhydrol.2006.02.036>
- 756 Niu, X.T., Fan, J., Du, M.G., Dai, Z.J., Luo, R.H., Yuan, H.Y., Zhang, S.G., 2023. Changes of Rainfall
757 Partitioning and canopy interception modeling after progressive thinning in two shrub plantations
758 on the Chinese Loess Plateau. *J. Hydrol.* 619, 129299.
759 <https://doi.org/10.1016/j.jhydrol.2023.129299>
- 760 [Pinos, J., Latron, J., Levia, D. F., Llorens, P., 2021. Drivers of the circumferential variation of stemflow](#)
761 [inputs on the boles of *Pinus sylvestris* L. \(Scots pine\). *Ecohydrology*, 14\(8\), e2348.](#)
- 762 Ponette-González, A.G., Weathers, K.C., Curran, L.M., 2010. Water inputs across a tropical montane
763 landscape in Veracruz, Mexico: synergistic effects of land cover, rain and fog seasonality, and
764 interannual precipitation variability. *Global Change Biol.* 16(3), 946–963.
765 <https://doi.org/10.1111/j.1365-2486.2009.01985.x>
- 766 Price, A.G., Dunham, K., Carleton, T., Band, L., 1997. Variability of water fluxes through the black
767 spruce (*Picea mariana*) canopy and feather moss (*Pleurozium schreberi*) carpet in the boreal forest
768 of Northern Manitoba. *J. Hydrol.* 196(1–4), 310–323. [https://doi.org/10.1016/S0022-](https://doi.org/10.1016/S0022-1694(96)03233-7)
769 1694(96)03233-7
- 770 Reynaert, S., De Boeck, H.J., Verbruggen, E., Verlinden, M., Flowers, N., Nijs, I., 2021. Risk of short-
771 term biodiversity loss under more persistent precipitation regimes. *Global Change Biol.* 27(8),
772 1614–1626. <https://doi.org/10.1111/gcb.15501>
- 773 Rodrigues, A.F., Terra, M.C., Mantovani, V.A., Cordeiro, N.G., Ribeiro, J.P., Guo, L., Nehren, U., Mello,
774 M.J., Mello, C.R., 2022. Throughfall spatial variability in a neotropical forest: Have we correctly
775 accounted for time stability? *J. Hydrol.* 608, 127632. <https://doi.org/10.1016/j.jhydrol.2022.127632>
- 776 Seiler, J., Matzner, E., 1995. Spatial variability of throughfall chemistry and selected soil properties as
777 influenced by stem distance in a mature Norway spruce (*Picea abies*, Karst.) stand. *Plant Soil* 176,
778 139–147. <https://doi.org/10.1007/BF00017684>
- 779 Shen, W.J., Ren, H.L., Jenerette, G.D., Hui, D.F., Ren, H., 2013. Atmospheric deposition and canopy
780 exchange of anions and cations in two plantation forests under acid rain influence. *Atmos Environ.*
781 64, 242–250. <https://doi.org/10.1016/j.atmosenv.2012.10.015>
- 782 Shinohara, Y., Levia, D.F., Komatsu, H., Nogata, M., Otsuki, K., 2015. Comparative modeling of the
783 effects of intensive thinning on canopy interception loss in a Japanese cedar (*Cryptomeria japonica*

784 D. Don) forest of western Japan. *Agric. For. Meteorol.* 214–215, 148–156.
785 <https://doi.org/10.1016/j.agrformet.2015.08.257>.

786 Siegert, C.M., Levia, D.F., 2014. Seasonal and meteorological effects on differential stemflow funneling
787 ratios for two deciduous tree species. *J. Hydrol.* 519, 446–454.
788 <https://doi.org/10.1016/j.jhydrol.2014.07.038>

789 Staelens, J., De Schrijver, A., Verheyen, K., 2007. Seasonal variation in throughfall and stemflow
790 chemistry beneath a European beech (*Fagus sylvatica*) tree in relation to canopy phenology. *Can. J.*
791 *Forest Res.* 37(8), 1359–1372. <https://doi.org/10.1139/X07-003>

792 Staelens, J., De Schrijver, A., Verheyen, K., Verhoest, N.E., 2006. Spatial variability and temporal
793 stability of throughfall deposition under beech (*Fagus sylvatica* L.) in relationship to canopy
794 structure. *Environ. Pollut.* 142(2), 254–263. <https://doi.org/10.1016/j.envpol.2005.10.002>

795 Su, L., Zhao, C.M., Xu, W.T., Xie, Z.Q., 2019. Hydrochemical fluxes in bulk precipitation, throughfall,
796 and stemflow in a mixed evergreen and deciduous broadleaved forest. *Forests* 10(6), 507.
797 <https://doi.org/10.3390/f10060507>

798 Sun, J.M., Yu, X.X., Wang, H.N., Jia, G.D., Zhao, Y., Tu, Z.H., Deng, W.P., Jia, J.B., Chen, J.G., 2018.
799 Effects of forest structure on hydrological processes in China. *J. Hydrol.* 561, 187–199.
800 <https://doi.org/10.1016/j.jhydrol.2018.04.003>

801 Sun, S.Y., Liu, X.F., Lu, S.X., Cao, P.L., Hui, D.F., Chen, J., Guo, J.F., Yang, Y.S., 2023. Depth-dependent
802 response of particulate and mineral-associated organic carbon to long-term throughfall reduction in
803 a subtropical natural forest. *Catena*, 223, 106904. <https://doi.org/10.1016/j.catena.2022.106904>

804 Tonello, K.C., Rosa, A.G., Pereira, L.C., Matus, G.N., Guandique, M.E.G., Navarrete, A.A., 2021a.
805 Rainfall partitioning in the Cerrado and its influence on net rainfall nutrient fluxes. *Agric. For.*
806 *Meteorol.* 303, 108372. <https://doi.org/10.1016/j.agrformet.2021.108372>

807 Tonello, K.C., Van Stan II, J.T., Rosa, A.G., Balbinot, L., Pereira, L.C., Bramorski, J., 2021b. Stemflow
808 variability across tree stem and canopy traits in the Brazilian Cerrado. *Agric. For. Meteorol.* 308,
809 108551. <https://doi.org/10.1016/j.agrformet.2021.108551>

810 Turpault, M.P., Kirchen, G., Calvaruso, C., Redon, P.O., Dincher, M., 2021. Exchanges of major elements
811 in a deciduous forest canopy. *Biogeochemistry*, 152, 51–71. <https://doi.org/10.1007/s10533-020-00732-0>

812

813 Wu, T., Song, Y.T., Tissue, D., Su, W., Luo, H.Y., Li, X., Yang, S.M., Liu, X.J., Yan J.H., Huang, J., Liu,
814 J.X., 2023. Photosynthetic and biochemical responses of four subtropical tree seedlings to reduced
815 dry season and increased wet season precipitation and variable N deposition. *Tree Physiol.* tpad114.

816 [Wu, Y.P., Yin, X.W., Zhou, G.Y., Bruijnzeel, L. A., Dai, A.G., Wang, F., Gentine, P., Zhang, G.C., Song,](https://doi.org/10.1038/s41467-023-44562-8)
817 [Y.N., Zhou, D.C., 2024. Rising rainfall intensity induces spatially divergent hydrological changes](https://doi.org/10.1038/s41467-023-44562-8)
818 [within a large river basin. *Nat. Commun.* 15\(1\), 823. <https://doi.org/10.1038/s41467-023-44562-8>](https://doi.org/10.1038/s41467-023-44562-8)

819 Van Stan II, J.T., Pypker, T.G., 2015. A review and evaluation of forest canopy epiphyte roles in the
820 partitioning and chemical alteration of precipitation. *Sci. Total Environ.* 536, 813–824.
821 <https://doi.org/10.1016/j.scitotenv.2015.07.134>

822 Van Stan, J.T., Wagner, S., Guillemette, F., Whitetree, A., Lewis, J., Silva, L., Stubbins, A., 2017.
823 Temporal dynamics in the concentration, flux, and optical properties of tree-derived dissolved

824 organic matter in an epiphyte-laden oak-cedar forest. *J. Geophys. Res-Bioge.* 122(11), 2982–2997.
825 <https://doi.org/10.1002/2017JG004111>

826 Wang, C.Y., Sun, X.C., Fan, C.B., Wei, Y.X., Jia, G.K., Cao, Y.H., 2023. Spatio-temporal variability and
827 intra-event variation of throughfall ammonium and nitrate in a pine plantation. *Hydrol. Process.*
828 e14872. <https://doi.org/10.1002/hyp.14872>

829 Yan, J.H., Zhou, G.Y., Zhang, D.Q., Wang, X., 2003. Spatial and temporal variations of some
830 hydrological factors in a climax forest ecosystem in the Dinghushan region. *Acta Ecologica Sinica*
831 23(11), 2359–2366. <https://europepmc.org/article/cba/534217>

832 Yue, K., De Frenne, P., Fornara, D.A., Van Meerbeek, K., Li, W., Peng, X., Ni, X.Y., Peng, Y., Wu, F.Z.,
833 Yang Y.S., Peñuelas, J., 2021. Global patterns and drivers of rainfall partitioning by trees and
834 shrubs. *Global Change Biol.* 27(14), 3350–3357. <https://doi.org/10.1111/gcb.15644>

835 Zabret, K., Rakovec, J., Šraj, M., 2018. Influence of meteorological variables on rainfall partitioning for
836 deciduous and coniferous tree species in urban area. *J. Hydrol.* 558, 29–41.
837 <https://doi.org/10.1016/j.jhydrol.2018.01.025>

838 Zhang, W.J., Zhu, X.A., Chen, C.F., Zeng, H.H., Jiang, X.J., Wu, J.E., Zou, X., Yang, B., Liu, W.J., 2021.
839 Large broad-leaved canopy of banana (*Musa nana* Lour.) induces dramatically high spatial–
840 temporal variability of throughfall. *Hydrol. Res.* 52(6), 1223–1238.
841 <https://doi.org/10.2166/nh.2021.023>

842 Zhang, Y.F., Wang, X.P., Hu, R., Pan, Y.X., Paradeloc, M., 2015. Rainfall partitioning into throughfall,
843 stemflow and interception loss by two xerophytic shrubs within a rain-fed re-vegetated desert
844 ecosystem, northwestern China. *J. Hydrol.* 527, 1084–1095.
845 <https://doi.org/10.1016/j.jhydrol.2015.05.060>

846 Zhang, Y.F., Yuan, C., Chen, N., Levia, D.F., 2023. Rainfall partitioning by vegetation in China: A
847 quantitative synthesis. *J. Hydrol.* 617, 128946. <https://doi.org/10.1016/j.jhydrol.2022.128946>

848 Zhao, W.Y., Ji, X.B., Jin, B.W., Du, Z.Y., Zhang, J.L., Jiao, D.D., Zhao, L.W., 2023. Experimental
849 partitioning of rainfall into throughfall, stemflow and interception loss by *Haloxylon ammodendron*,
850 a dominant sand-stabilizing shrub in northwestern China. *Sci. Total Environ.* 858, 159928.
851 <https://doi.org/10.1016/j.scitotenv.2022.159928>

852 Zheng, M.H., Zhang, T., Luo, Y.Q., Liu, J.X., Lu, X.K., Ye, Q., Wang, S.H., Huang, J., Mao, Q.G., Mo,
853 J.M., Zhang, W., 2022. Temporal patterns of soil carbon emission in tropical forests under long-term
854 nitrogen deposition. *Nat. Geosci.* 15, 1002–1010. <https://doi.org/10.1038/s41561-022-01080-4>

855 Zhou, G.Y., Wei, X.H., Wu, Y.P., Liu, S.G., Huang, Y.H., Yan, J.H., Zhang, D.Q., Zhang, Q.M., Liu, J.X.,
856 Meng, Z., Wang, C.L., Chu, G.W., Liu, S.Z., Tang, X.L., Liu, X.D., 2011. Quantifying the
857 hydrological responses to climate change in an intact forested small watershed in Southern China.
858 *Global Change Biol.* 17(12), 3736–3746. <https://doi.org/10.1111/j.1365-2486.2011.02499.x>

859 Ziegler, A.D., Giambelluca, T.W., Nullet, M.A., Sutherland, R.A., Tantasarin, C., Vogler, J.B., Negishi,
860 J.N., 2009. Throughfall in an evergreen-dominated forest stand in Northern Thailand: comparison
861 of mobile and stationary methods. *Agric. For. Meteorol.* 149, 373–384.
862 <https://doi.org/10.1016/j.agrformet.2008.09.002>.

863 Zimmermann, A., Wilcke, W., Elsenbeer, H., 2007. Spatial and temporal patterns of throughfall quantity

864 and quality in a tropical montane forest in Ecuador. *J. hydrol.* 343(1–2), 80–96.
865 <https://doi.org/10.1016/j.jhydrol.2007.06.012>

866 **Tables**

867

868 **Table 1** Correlations between throughfall and stemflow and rainfall and forest factors

	Gross rainfall	DBH	CA	Height	LAI
Throughfall	0.72***	—	—	—	-0.58**
stemflow	0.77***	0.65*	-0.75**	0.54**	-0.55**

869 DBH: diameter at breast height; CA: crown area; LAI: leaf area index. * $P < 0.05$, ** $P < 0.01$, *** $P <$

870 0.001

871

872

873

874

875

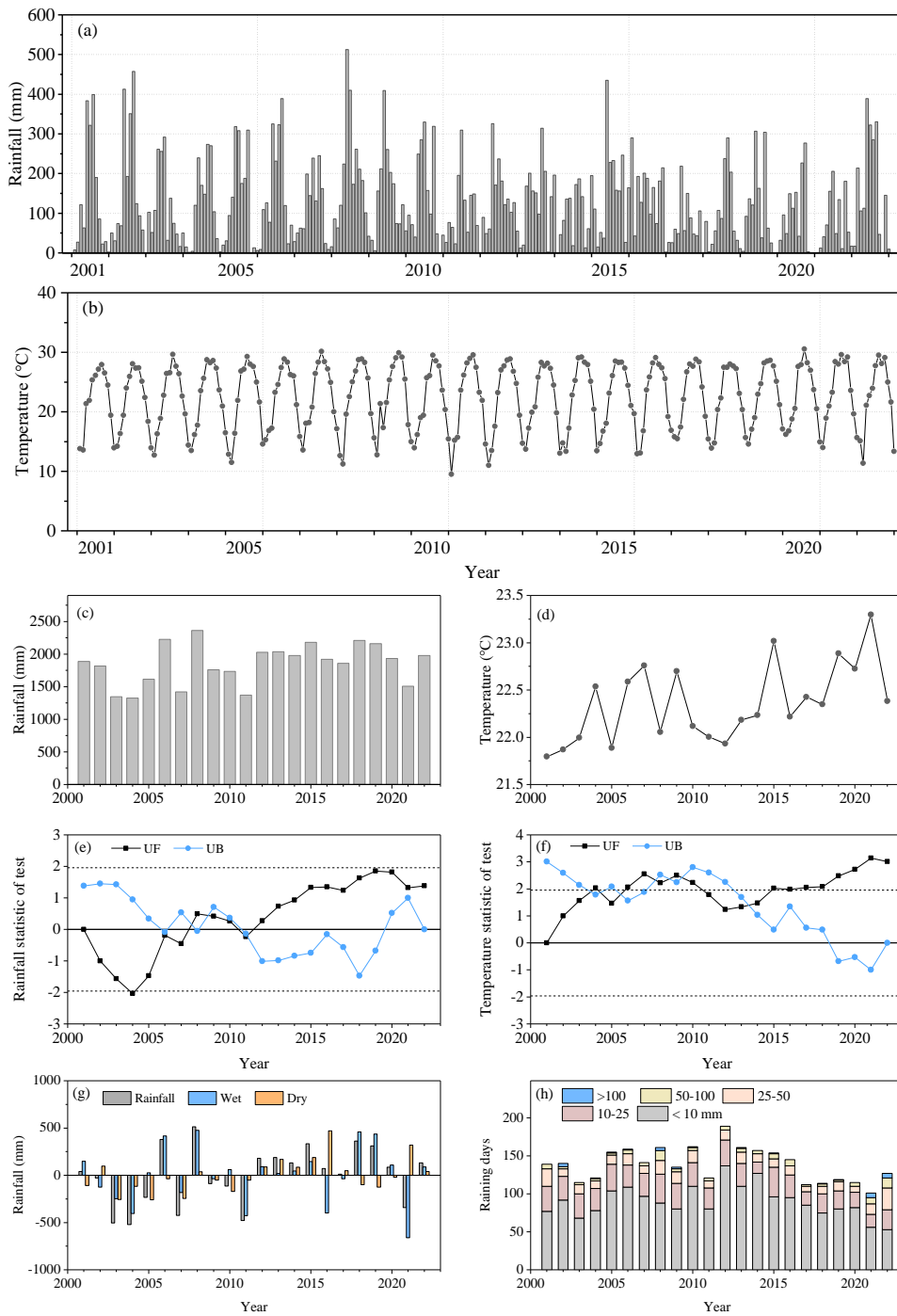
876

877 **Table 2** Analysis of variance (ANOVA) for throughfall and stemflow affected by rainfall
878 classifications and tree species

Summary of ANOVA	Throughfall		Stemflow
Rainfall classification (R)	< 0.05	Rainfall classification (R)	< 0.001
Forest type (F)	< 0.001	Tree species (T)	< 0.001
R × F	0.861	R × T	< 0.001

879 $\alpha = 0.05$

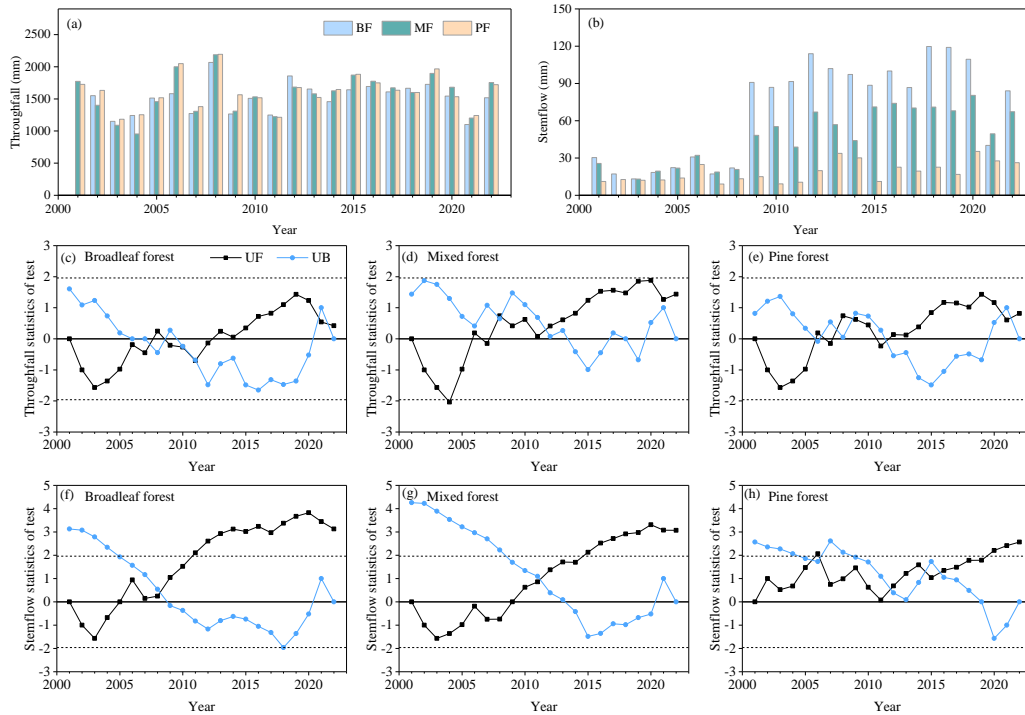
880



882

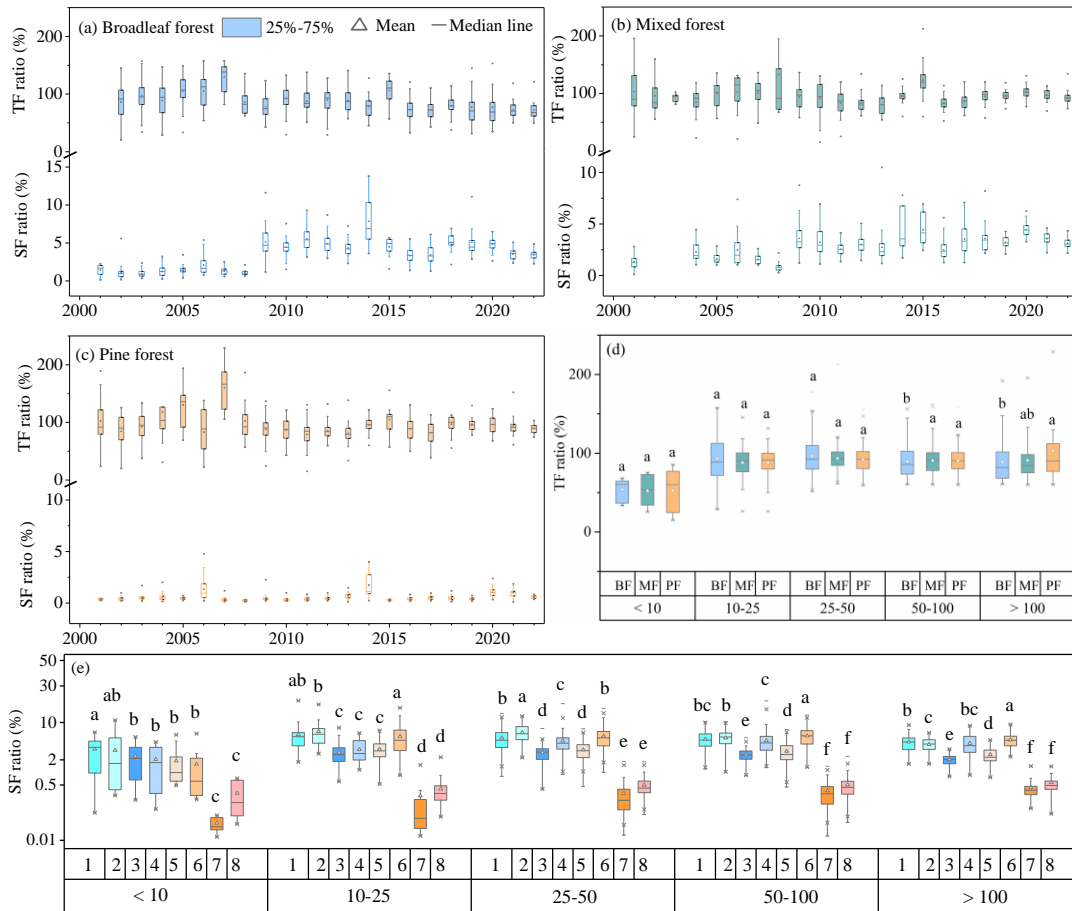
883 **Fig. 1** (a) and (b) rainfall and temperature in Dinghushan Biosphere Reserve in Southern China
 884 from 2001–2022, (c) and (d) annual rainfall and temperature, (e) and (f) rainfall and
 885 temperature statistic of Mann-Kendall test, respectively. (g) Anomaly of annual rainfall from
 886 2001–2022, (h) annual raining days in five classifications. UF (Unadjusted Forward) > 0
 887 indicate a continuous increasing trend ($P < 0.05$). The intersection points of UF and UB
 888 (Unadjusted Backward) is the mutation time point. Within the confidence interval [-1.96, 1.96],
 889 the variable presents a significantly mutation growth state at this time point ($P < 0.05$).

890



891

892 **Fig. 2** (a) and (b) Annual throughfall and stemflow in the broadleaf forest (BF), mixed pine and
 893 broadleaf forest (MF) and pine forest (PF) from 2001–2022, respectively, (c) ~ (h) rainfall and
 894 stemflow statistic of Mann-Kendall test, respectively. UF (Unadjusted Forward) > 0 indicate a
 895 continuous increasing trend ($P < 0.05$). The intersection points of UF and UB (Unadjusted
 896 Backward) is the mutation time point. Within the confidence interval $[-1.96, 1.96]$, the variable
 897 presents a significantly mutation growth state at this time point ($P < 0.05$).



898

899

Fig. 3 Box plots of throughfall ratio and stemflow ratio in (a) broadleaf forest, (b) mixed pine and broadleaf forest and (c) pine forest from 2001–2022. Boxed plots of (d) TF ratio in the three forests and (e) SF ratio for eight plant species based on the rainfall classifications (broadleaf forest: *Acmena acuminatissima* (Blume) Merr. et Perry (SF1), *Cryptocarya chinensis* (Hance) Hemsl. (SF2), *Gironniera subaequalis* Planch. (SF3), *Schima superba* Gardn. et Champ. (SF4); mixed forest: *Castanea henryi* (Skam) Rehd. et Wils. (SF5), *Schima superba* Gardn. et Champ. (SF6), *Pinus massoniana* Lamb. (SF7); pine forest: *Pinus massoniana* Lamb. (SF8). Different letters indicate a significant difference at $P < 0.05$

900

901

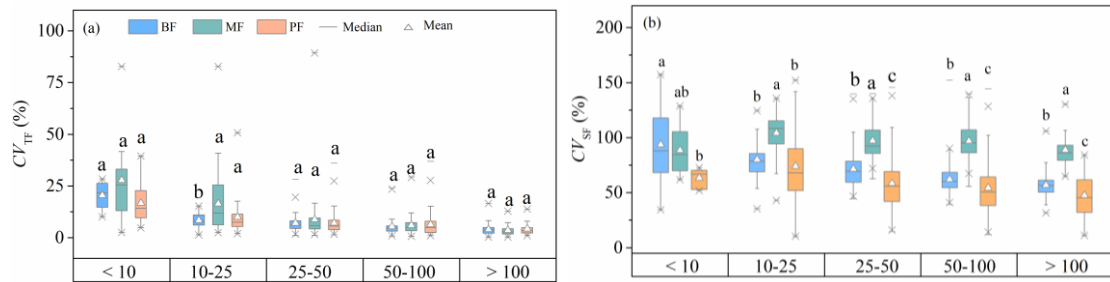
902

903

904

905

906



908

909

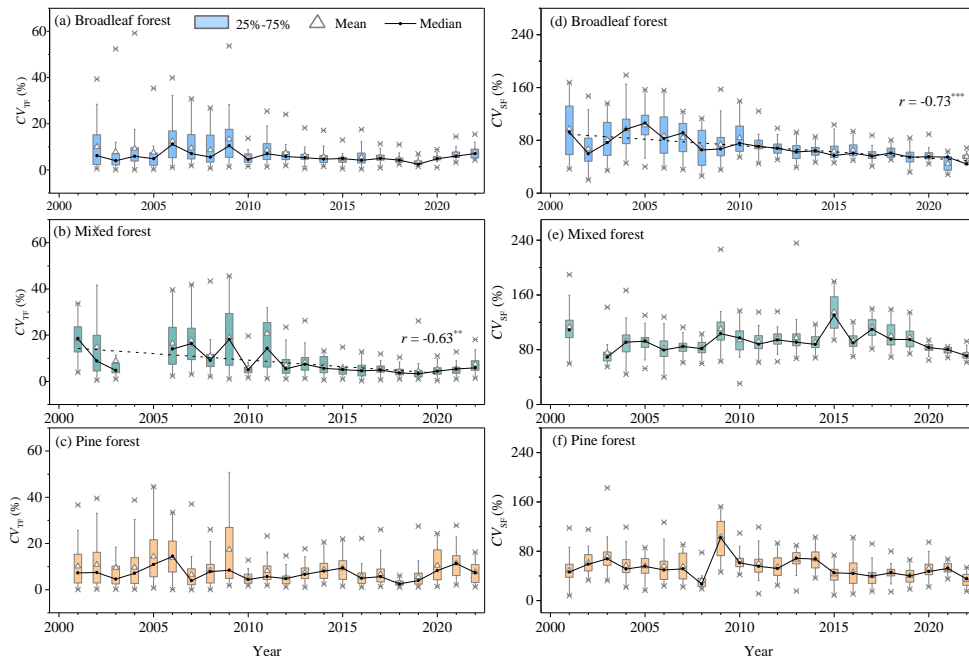
Fig. 4 Box plots of coefficient of variation (CV , %) in (a) throughfall (TF) and (b) stemflow (SF) in

910

broadleaf forest (BF), mixed pine and broadleaf forest (MF) and pine forest (PF) based on the

911

rainfall classifications. Different letters indicate a significant difference at $P < 0.05$



913

914

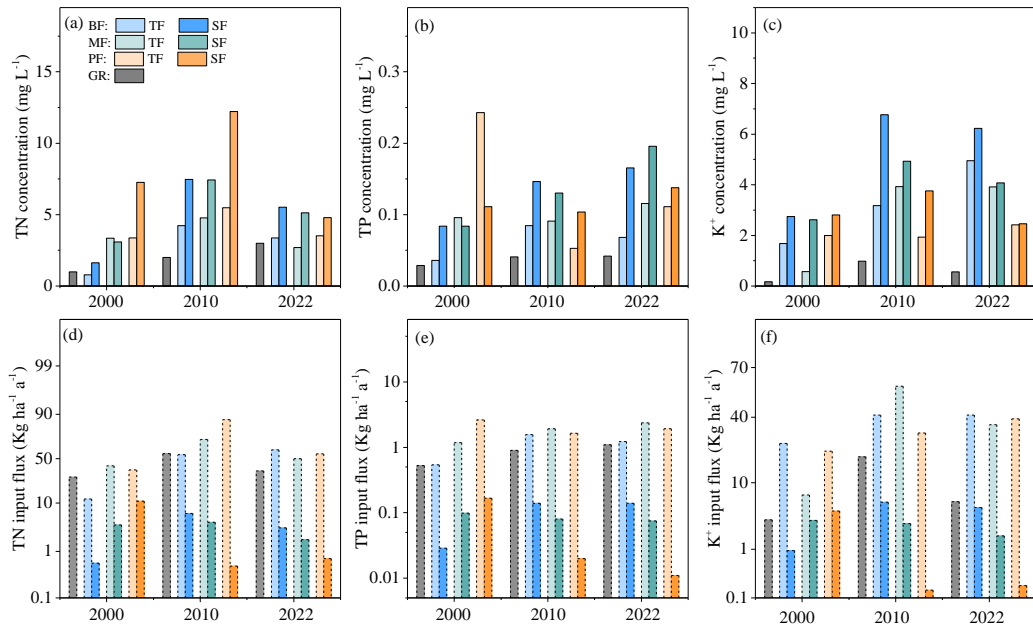
Fig. 5 Box plots of coefficient of variation (CV , %) in (a, b, and c) throughfall (TF) and (d, e, and f)

915

stemflow (SF) in the three forests from 2001 to 2022. Medians of annual CV were fitted. r :

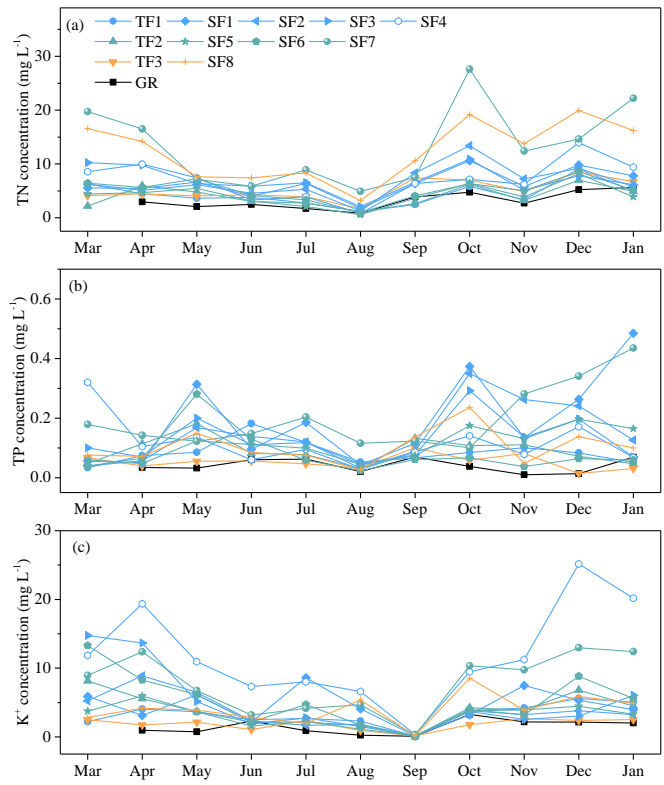
916

Pearson coefficient of correlation; *: $P < 0.05$, **: $P < 0.01$, ***: $P < 0.001$



917

918 **Fig. 6** Concentrations and fluxes of TN, TP and K⁺ of gross rainfall (GR), throughfall (TF) and
 919 stemflow (SF) in the broadleaf forest (BF), mixed forest (MF) and pine forest (PF) in 2000,
 920 2010 and 2022, respectively.



921
 922 **Fig. 7** Monthly concentrations of (a) TN, (b) TP and (c) K⁺ of throughfall (TF1) and stemflow (SF1,
 923 SF2, SF3 and SF4) in the broadleaf forest, throughfall (TF2) and stemflow (SF5, SF6 and SF7)
 924 in the mixed forest, throughfall (TF3) and stemflow (SF8) in the pine forest.

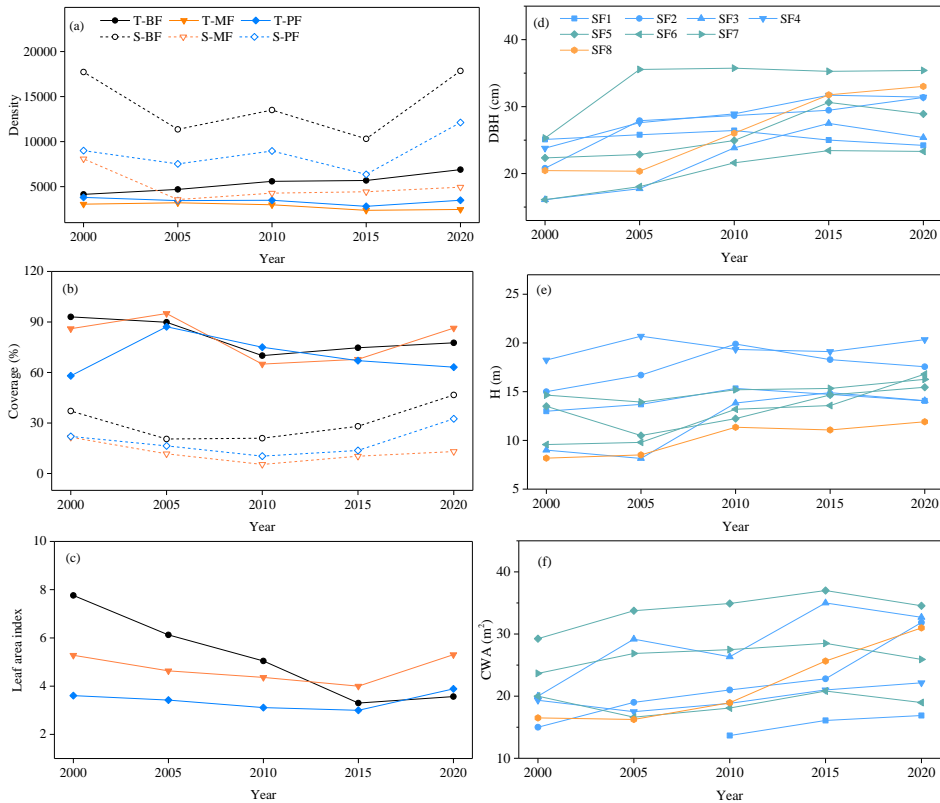


Fig. 8 Plant density, canopy coverage and leaf area index of tree (T) and shrub (S) in the broadleaf forest (BF), mixed forest (MF) and pine forest (PF), respectively. Diameter at breast height (DBH), height (H) and crown area (CA) is given for eight stemflow-sampled trees, respectively. Tree height was measured using laser range finder. Tape measure was used to measure the diameter of trees at a height of 1.3 m, namely DBH (diameter at breast height). CA (crown area): the laser rangefinder was used to measure the maximum diameter at the edge of the canopy, with multiple measurements at different points to ensure accuracy. Plant density: 25 plots of 20 m × 20 m (A1-A25 plots) were built on a plot of 1hm² to survey tree density. Then, 25 plots of 5 m × 5 m (B1-B25 plots) were randomly set on the A1-A25 plots to survey shrub density. Finally, 25 plots of 1 m × 1 m (C1-C25 plots) were randomly set on the B1-B25 plots to survey herb density. Canopy coverage: 25 observation plots (1 m × 1 m) were selected in the 1 hm² area of each forest type. The percentage of the surface area covered by plants to the total plot area is termed canopy coverage (%). LAI (Leaf area index) was measured using a LAI-2200 plant canopy analyzer with 90° view caps (Li-Cor Inc., USA). 10 observation points (distance about 10 m) were selected in the 1 hm² area of each forest type with 5 replications.

925
 926
 927
 928
 929
 930
 931
 932
 933
 934
 935
 936
 937
 938
 939
 940
 941